



OPEN

# Reduced neuronal signaling in the ageing apolipoprotein-E4 targeted replacement female mice

SUBJECT AREAS:

MOLECULAR  
NEUROSCIENCE

NEURAL AGEING

Shan-May Yong<sup>1</sup>, Mei-Li Lim<sup>1</sup>, Chian-Ming Low<sup>2</sup> & Boon-Seng Wong<sup>1</sup>Received  
2 April 2014Accepted  
16 September 2014Published  
10 October 2014Correspondence and  
requests for materials  
should be addressed to  
B.-S.W. (bswong@nus.  
edu.sg)<sup>1</sup>Department of Physiology, Yong Loo Lin School of Medicine, National University of Singapore, Singapore, <sup>2</sup>Department of Pharmacology, Yong Loo Lin School of Medicine, National University of Singapore, Singapore.

The effect of ApoE on NMDAR-dependent ERK/CREB signaling is isoform-dependent, and ApoE4 accelerates memory decline in ageing. However, this isoform-dependent function on neuronal signaling during ageing is unclear. In this study, we have examined NMDAR-associated ERK/CREB signal transduction in young and aged huApoE3 and huApoE4 targeted replacement (TR) mice. At 12 weeks huApoE4 mouse brain, increased NR1-S896 phosphorylation was linked to higher protein kinase C (PKC) activation. This up-regulation was accompanied by higher phosphorylation of AMPA GluR1-S831, CaMKII, ERK1/2 and CREB. But at 32 weeks, there was no significant difference between huApoE3 and huApoE4 TR mice on NMDAR-associated ERK/CREB signaling. Interestingly, in 72-week-old huApoE4 TR mice, protein phosphorylation that were increased in younger mice were significantly reduced. Lower NR1-S896 phosphorylation was linked to reduced PKC, GluR1-S831, CaMKII, ERK1/2 and CREB phosphorylation in huApoE4 TR mice as compared to huApoE3 TR mice. Furthermore, we have consistently detected lower ApoE levels in young and aged huApoE4 TR mouse brain, and this was associated with reduced expression of the ApoE receptor, LRP1 and NR2A-Y1246 phosphorylation. These results suggest age-specific, isoform-dependent effects of ApoE on neuronal signaling.

The human apolipoprotein E (apoE) gene is genetically linked to cognitive function in ageing and diseases<sup>1-4</sup>. This gene is located on chromosome 19 encoding a 35 kDa protein<sup>5</sup> that exists in 3 isoforms, E2, E3 and E4<sup>6</sup>. These isoforms differ by amino acid substitutions at two positions (residues 112 and 158): E2 (Cys<sup>112</sup>, Cys<sup>158</sup>), E3 (Cys<sup>112</sup>, Arg<sup>158</sup>), and E4 (Arg<sup>112</sup>, Arg<sup>158</sup>). The ApoE3 allele is maintained at an allele frequency of ~78% in populations and the ApoE4 has an allele frequency of ~14% in the populations. The ApoE2 allele however is relatively rare, existing in <10% in most populations.

ApoE is highly expressed in the liver and brain<sup>7</sup>. Non-demented aged ApoE4 carriers are reported to experience faster cognitive decline<sup>1-4</sup>. Similar impairment is also observed in mice expressing human ApoE4<sup>7,8</sup>.

In the central nervous system (CNS), ApoE binds to the highly conserved low-density lipoprotein receptor (LDLR) family<sup>9</sup>, including LRP1 and ApoER2. This LDLR family is intimately involved in neuronal signal transduction, modulation of ligand-gated ion channels, and regulating neurite outgrowth, synapse formation and neuronal migration<sup>10</sup>.

The ApoE isoform-dependent effect on cognition is linked to the *N*-methyl-D-aspartate receptor (NMDAR)<sup>11-13</sup> since ApoER2 was reported to bind NMDAR1 (NR1). Disrupting the binding of reelin, an ApoER2 ligand, results in learning and memory defects<sup>14</sup>. Another ApoE receptor, LRP1, is able to regulate NMDA-dependent Ca<sup>2+</sup> influx possibly via scaffolding protein PSD95<sup>15</sup>.

NMDARs are glutamate-gated ion channels comprising an assembly of three major subunits<sup>16</sup> that are pivotal for learning and memory, and the induction of long-term synaptic plasticity. Changes in NMDAR subunits composition and localization have been detected during ageing<sup>17,18</sup>. NMDAR function is mediated by calcium (Ca<sup>2+</sup>) ions leading to the intracellular activation of the transcription factor cAMP/calcium-dependent response element binding partner (CREB)<sup>16,19,20</sup>. The function of NMDAR is closely associated with AMPAR activation<sup>21,22</sup>. Neurons expressing ApoE4 were reported to have lower NMDAR and AMPAR functions<sup>23</sup>, leading to lower LTP<sup>13</sup>.

ApoE has been shown to regulate the NMDAR-dependent ERK/CREB signaling<sup>24</sup>, and this process is ApoE isoform-dependent<sup>13</sup>. Although ApoE4 accelerates memory decline in ageing, these studies did not examine if and how ApoE isoforms interact with these signaling proteins during ageing. Hence, our study will investigate this



isoform-dependent change in NMDAR-associated ERK-CREB signaling in the ageing huApoE3 and huApoE4 targeted replacement (TR) mice.

## Results

**ApoE expression in the ageing huApoE TR mouse brain.** We and others have observed lower ApoE levels in the brain of young and aged huApoE4 TR mice<sup>25–27</sup> and in non-demented APOE4 carriers<sup>27</sup>. However, it is unclear how lower ApoE4 content (Figures 1 and S1) could affect the expression of ApoE receptor.

To examine this relationship, we immunoblotted for the ApoE receptor, ApoER2 as this protein was reported to bind NMDAR1 (NR1)<sup>11</sup>. However, we were unable to detect this protein in both huApoE3 and huApoE4 TR mice. We next probed for another ApoE receptor, the low-density lipoprotein receptor-related protein 1 (LRP1)<sup>9</sup> in the ageing brain of huApoE3 and huApoE4 TR mice. By comparing the protein level at each time point, we found that LRP1 content was reduced by 27%, 27% and 36% in the brains of huApoE4 TR mice at 12, 32 and 72 weeks as compared to huApoE3 TR mice of similar ages (Figures 1 and S1). On the other hand, ApoE level was reduced by 37%, 29% and 24% in the brain of huApoE4 TR mice as compared to huApoE3 TR mice at 12, 32 and 72 weeks respectively (Figures 1 and S1).

**Differential NR1 phosphorylation in ageing brain of ApoE TR mice.** ApoE4 was reported to impair synaptic plasticity by reducing *N*-methyl-D-aspartate receptor (NMDAR) function<sup>12,13,24</sup>. NMDAR1 (NR1) is the obligatory subunit of the heterotetramer receptor<sup>16</sup>. We therefore examined the effect of lower ApoE4 expression on NR1 activation.

NR1 phosphorylation at S896 was significantly increased (~154%) in 12-week-old huApoE4 TR mice as compared to huApoE3 TR mice (Figures 2 and S2). At 32 weeks, there was no difference in NR1-S896 phosphorylation between huApoE3 and huApoE4 TR mice. However, at 72 weeks, NR1-S896 phosphorylation was reduced by 40% in huApoE4 TR mice.

In contrast, there was no difference in NR1 phosphorylation at S897 between huApoE3 and huApoE4 TR mice at 12, 32, and 72 weeks (Figures 2 and S2).

**NR2A phosphorylation was lowered in the brain of huApoE4 TR mice.** NR2 is another major subunit of the NMDAR<sup>28</sup>. While the NR1 subunit is expressed ubiquitously, NR2 expression is spatially and temporally regulated. NR2A and NR2B are the predominant NR2 subunits expressed in the cortex and hippocampus<sup>16</sup>.

In figures 3 and S3, NR2A and NR2B levels did not differ between huApoE3 and huApoE4 TR mice at 12, 32 and 72 weeks. On the other hand, NR2A phosphorylation at Y1246 was significantly

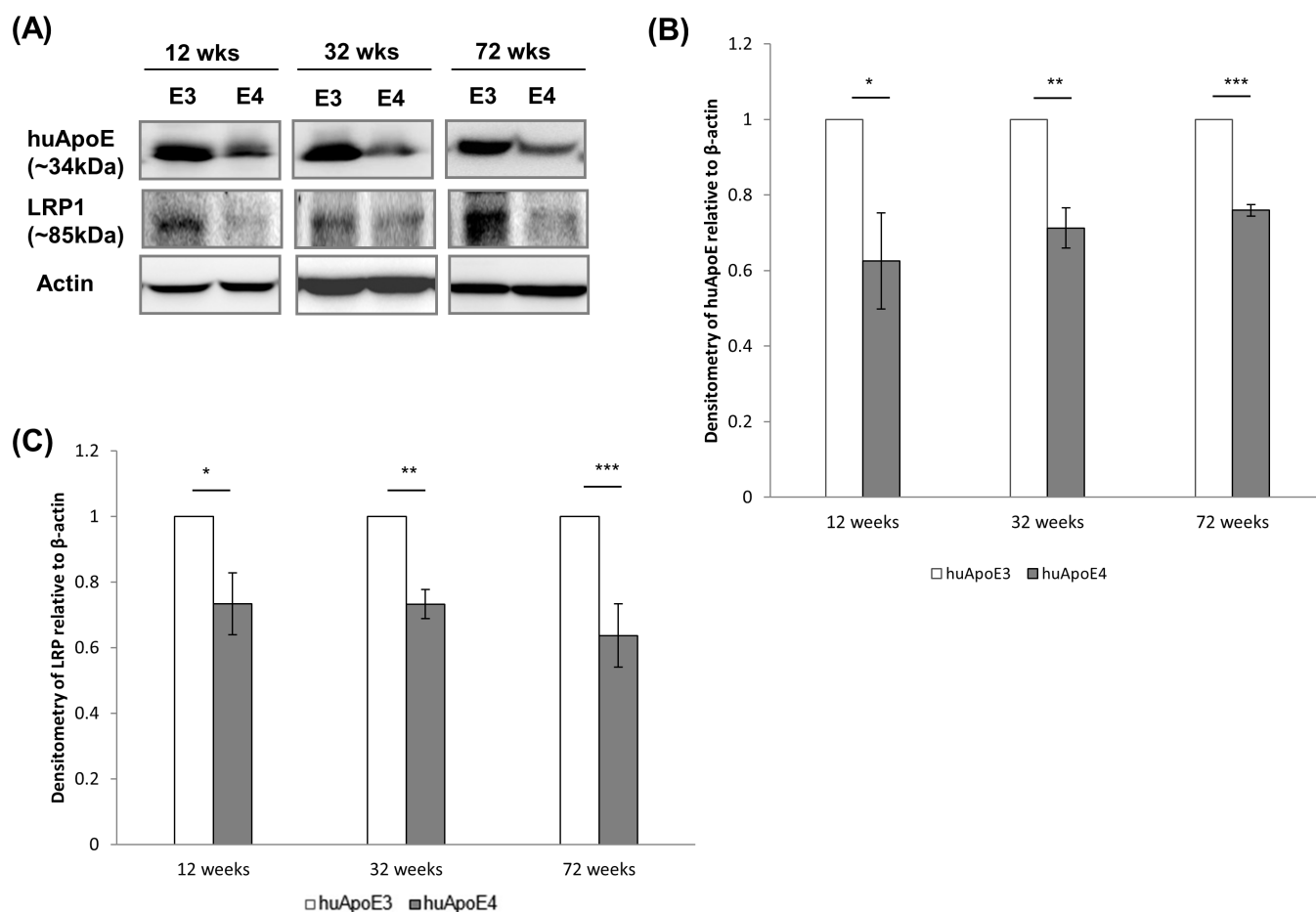


**Figure 1 | Lower human apolipoprotein E (huApoE) and LRP1 levels in the brain of huApoE4 targeted replacement (TR) mice as compared to huApoE3 TR mice.** Western blot and densitometric analysis of huApoE and LRP1 levels in E3 (white bar) and E4 (grey bar) TR mice at 12, 32 and 72 weeks of age. (A) The blot shown here is a representative of five independent experiments. Blot images were cropped for comparison. Actin was used as a loading control in each sample. (B, C) Densitometric analysis was performed using the NIH ImageJ software and the relative value for ApoE4 TR mice was normalized against age-matched ApoE3 TR mice. Each value represents the mean  $\pm$  SEM for individual mouse brain sample. Brain huApoE and LRP1 levels were significantly reduced in E4 TR mice as compared to E3 TR mice of similar age; (B) \*p = 0.001, \*\*p = 0.007, \*\*\*p < 0.001 using Student's t-test; (C) \*p = 0.01, \*\*p = 0.02, \*\*\*p = 0.003 using Student's t-test.

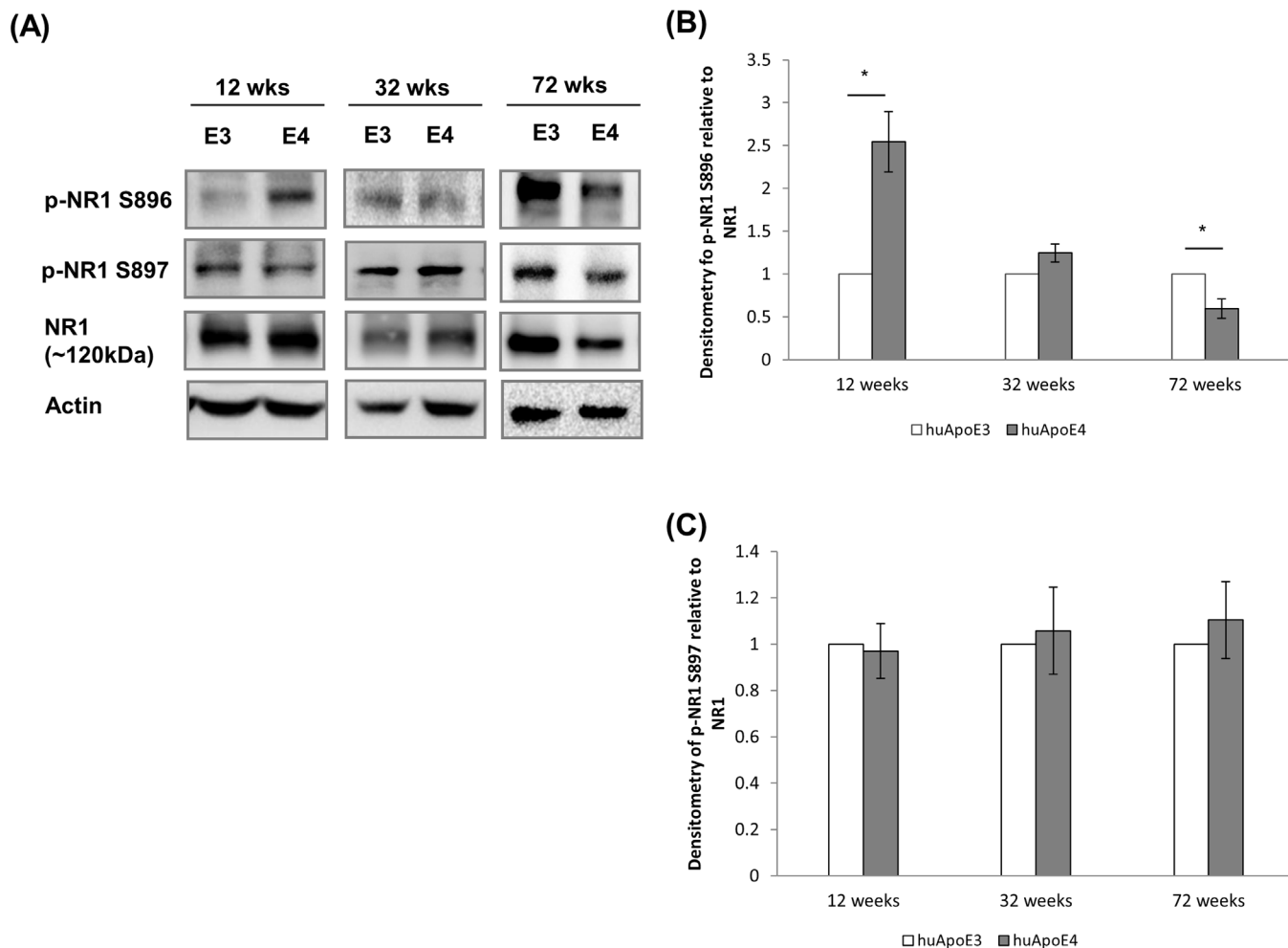


**Figure 2 | NR1 expression and phosphorylation in the ageing brain of huApoE TR mice.** Immunoblotting and densitometric analysis of total NMDA Receptor subunit 1 (NR1), phosphorylated NR1 at (S896) and (S897) in huApoE3 (white bar) and huApoE4 (grey bar) TR mice at 12, 32 and 72 weeks of age. (A) The blot shown here is a representative of five independent experiments. Blot images were cropped for comparison. (B, C) Densitometric analysis was performed using the NIH ImageJ software and the relative value for ApoE4 TR mice was normalized against age-matched ApoE3 TR mice. Each value represents the mean  $\pm$  SEM for individual mouse brain sample. In E4 TR mice, NR1 phosphorylation at S896 was significantly increased at 12 week but was significantly reduced at 72 week as compared to E3 TR mice of similar age (\* $p = 0.002$  using Student's *t*-test).

reduced in huApoE4 TR mice by 65%, 32% and 51% at 12, 32 and 72 weeks respectively as compared to huApoE3 TR mice. However, we were unable to detect NR2B phosphorylation at Y1472 in the huApoE TR mouse brain.

**Protein kinase C but not protein kinase A phosphorylation was altered in huApoE4 TR mice.** NR1 phosphorylation on S896 was reported to be regulated by protein kinase C (PKC), whereas NR1 phosphorylation on S897 was regulated by protein kinase A (PKA)<sup>29</sup>.

PKA is a heterotetramer composed of a regulatory subunit dimer and a catalytic subunit dimer<sup>30</sup>. The catalytic subunit can be spliced into three isoforms (C $\alpha$ , C $\beta$ , C $\gamma$ ). In figures 4 and S4, PKA phosphorylation at T197 on the C $\alpha$  subunit was not significantly affected between huApoE3 and huApoE4 TR mice. This is expected since NR1-S897 phosphorylation did not differ between huApoE3 and huApoE4 mice (Figure 2).

On the other hand, PKC has more than 12 different isoforms. The PKC isoforms are serine/threonine kinases involved in wide range of physiological processes including differentiation and brain function<sup>31</sup>. PKC  $\alpha$  isoform (PKC  $\alpha$ ) is ubiquitously expressed and is activated in response to many different kinds of stimuli. Here, we detected PKC phosphorylation at T497 on the  $\alpha$  subunit which was significantly increased by 49% in 12-week-old huApoE4 TR mice as

compared to age-matched huApoE3 TR mice (Figures 4 and S4). But at 72 weeks, PKC phosphorylation was reduced by 28% in huApoE4 TR mice as compared to huApoE3 TR mice. This change in profile is similar to that detected on NR1-S896 phosphorylation (Figure 2).

**Differential AMPA GluR1 phosphorylation in huApoE TR mice.** Another major glutamate receptor that exists alongside NMDAR is AMPA receptor (AMPA)<sup>16</sup>. Changes in NMDAR phosphorylation therefore could regulate AMPAR activity<sup>21,22</sup>.

In figures 5 and S5, AMPA GluR1 phosphorylation at S831 was increased by 44% in 12-week-old huApoE4 TR mice as compared to huApoE3 TR mice at similar age. However, when the mice were 72 weeks old, GluR1 S831 phosphorylation was significantly reduced by 34% in huApoE4 TR mice. When both huApoE3 and huApoE4 TR mouse brain samples from the three time points were examined in similar blot, there was an increased in GluR1 S831 phosphorylation in huApoE3 TR mice at 12- and 32-week (Figure S5).

In contrast, GluR1 phosphorylation at S845 did not differ between huApoE3 and huApoE4 TR mice at the three time points; 12, 32 and 72 weeks (Figure 5). This is expected as PKA regulates GluR1 phosphorylation at S845<sup>32</sup>, and PKA phosphorylation did not differ between huApoE3 and huApoE4 mice (Figure 4).

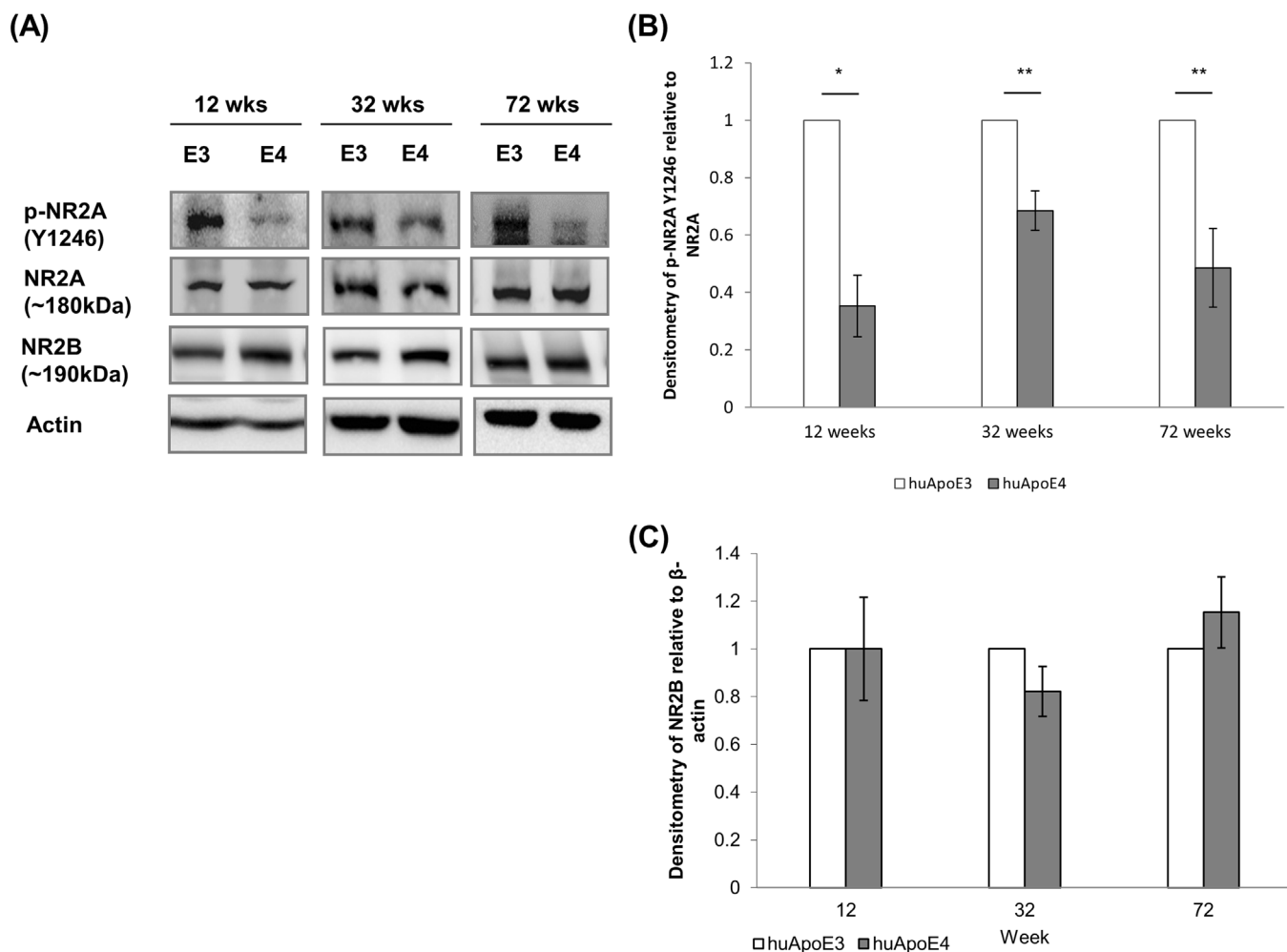


**Figure 3 | NR2 subunits expression and phosphorylation in the brain of huApoE4 TR mice as compared to huApoE3 TR mice.** Immunoblotting and densitometric analysis of NMDA Receptor subunit 2A and 2B (NR2A and NR2B), phosphorylated NR2A at (Y1246) in E3 (white bar) and E4 (grey bar) TR mice at 12, 32 and 72 weeks of age. (A) The blot is a representative of five independent experiments. Blot images were cropped for comparison. (B, C) Densitometric analysis was performed using the NIH ImageJ software and the relative value for ApoE4 TR mice was normalized against age-matched ApoE3 TR mice. Each value represents the mean  $\pm$  SEM for individual mouse brain sample. (B) NR2A phosphorylation at Y1246 levels in E4 TR mice were significantly reduced as compared to E3 TR mice (\* $p = 0.003$ , \*\* $p < 0.001$  using Student's t-test).

**CaMKII activation in the ageing huApoE TR mice.** ApoE effect on NMDAR function requires calcium ( $\text{Ca}^{2+}$ ) signaling<sup>33</sup>. The secondary messenger effects of  $\text{Ca}^{2+}$  are mostly mediated via  $\text{Ca}^{2+}$ -sensing protein kinases such as calmodulin kinase II (CaMKII)<sup>34</sup> that is able to dock with NMDAR. CaMKII has catalytic and regulatory domains. The binding of  $\text{Ca}^{2+}$  to its regulatory domain activates the kinase by phosphorylating threonine 286 (T286)<sup>35</sup>.

At 12 weeks, CaMKII phosphorylation was significantly increased by  $\sim 40\%$  in huApoE4 TR mice as compared to huApoE3 TR mice (Figures 6 and S6). In aged (72 weeks) mice, CaMKII phosphorylation was reduced by  $\sim 20\%$  in huApoE4 TR mice.

**ERK/CREB signaling in the ageing huApoE TR mice.** A major signaling cascades regulated by  $\text{Ca}^{2+}$  influx through NMDAR is the downstream extracellular signal-regulated kinase (ERK) pathway, which culminates in CREB-mediated gene transcription to influence neuronal survival and plasticity<sup>36–38</sup>.

ERK proteins are regulated by the dual phosphorylation of threonine 202 (T202) and tyrosine 204 (Y204) on ERK1 and, threonine 185 (T185) and tyrosine 187 (Y187) on ERK2<sup>39</sup>. In 12-week-old huApoE4 TR mice, ERK phosphorylation was significantly higher ( $\sim 167\%$ ) than huApoE3 TR mice (Figures 6 and S6). At 32 weeks, ERK phosphorylation did not differ between huApoE4 and huApoE3

TR mice. However, ERK phosphorylation in huApoE4 TR mice was reduced by 25% as compared to huApoE3 TR mice at 72 weeks.

Similar changes were observed in CREB signaling. CREB is activated by phosphorylation at Serine 133 (S133) by several signaling pathways including ERK<sup>38</sup>. In 12-week-old huApoE4 TR mice, CREB phosphorylation at S133 was increased by  $\sim 71\%$  as compared to huApoE3 TR mice (Figures 6 and S6). At 32 weeks, we did not detect any difference in CREB phosphorylation between the two mouse lines. But, at 72 weeks, CREB phosphorylation was reduced by  $\sim 30\%$  in huApoE4 TR mice as compared to huApoE3 TR mice.

## Discussion

The huApoE targeted replacement (TR) mice (apoE TR) are commonly used to examine the role of ApoE in memory formation and synaptic function<sup>8,40,41</sup>, due to the high degree of conservation between murine and human ApoE receptors<sup>9,42</sup>. ApoE4 TR mice are reported to have impaired spatial memory retention in tests that ApoE3 TR and murine apoE-expressing animals are able to perform<sup>8,40,43</sup>. The earlier studies have also observed gender susceptibility since the cognition of female ApoE4 mice is more affected than male ApoE4 mice<sup>8,40,43,44</sup>.

Most studies have reported cognitive impairment in aged huApoE TR mice at 15–18 months ( $\sim 65$ –78 weeks)<sup>8,40,41</sup>. However, there has

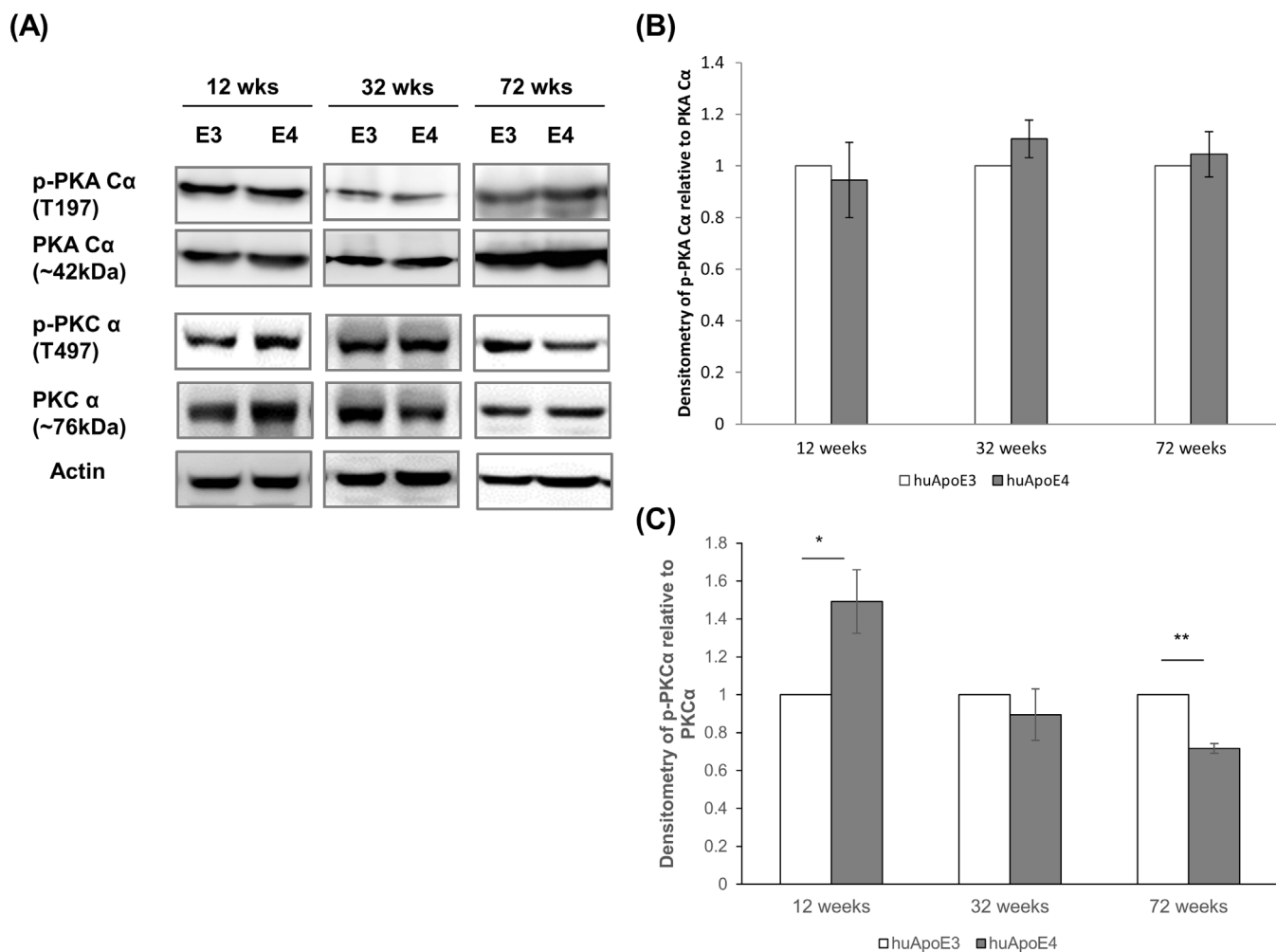


**Figure 4** | PKC but not PKA phosphorylation was altered in the brain of huApoE4 TR mice. Immunoblotting of protein kinase A C $\alpha$  subunit (PKA C $\alpha$ ) and protein kinase C  $\alpha$  subunit (PKC  $\alpha$ ) expression and phosphorylation in E3 (white bar) and E4 (grey bar) TR mice at 12, 32 and 72 weeks of age. (A) The blot shown here is a representative of five independent experiments. Blot images were cropped for comparison. (B, C) Densitometric analysis of phosphorylated PKA C $\alpha$  (T197) and PKC  $\alpha$  (T497) was performed using the NIH ImageJ software. The relative value for ApoE4 TR mice was normalized against age-matched ApoE3 TR mice. Each value represents the mean  $\pm$  SEM for individual mouse brain sample. (C) Brain PKC  $\alpha$  phosphorylation at T497 in E4 TR mice was significantly increased at 12 week but was significant reduced at 72 week as compared to E3 TR mice of similar age (\* $p = 0.03$ , \*\* $p < 0.001$  using Student's t-test).

been contrasting results on cognitive performance in young animals. In younger mice aged 6–8 months (~26–34 weeks), there was a report showing enhanced cognitive function in ApoE4 TR mice<sup>45</sup>, whereas another study observed impaired cognition in similar mouse line<sup>43</sup>.

To better understand the role of ApoE on neuronal signaling during development and ageing, we have chosen to examine and compare huApoE3 and huApoE4 TR female mice at 12, 32 and 72 weeks. In this study, we found that ApoE4 expression has differential effects on neuronal signaling in young and aged mice. In young mice (12 weeks), ApoE4 expression was linked to higher NMDAR-dependent ERK/CREB signaling. But at 32 weeks, there was no significant difference in the affected signaling pathways between huApoE3 and huApoE4 mice. However, in aged (72 weeks) mice, the signal transduction was lowered.

One possible explanations for our observations could be related to the structural difference between huApoE3 and huApoE4<sup>46</sup>. In huApoE4, arginine at position 112 mediates an intramolecular domain interaction between arginine at position 61 and glutamine at position 255. This intramolecular interaction however is absent in huApoE3 as the protein contains a cysteine at position 112. Another

possibility may be due to the lower ApoE levels reported in the brain of huApoE4 TR mice<sup>25–27</sup> and this could affect ApoE function on neuronal signaling.

The ApoE receptor ApoER2 has been shown to bind to NMDAR via PSD95<sup>11</sup>. In this study, we were unable to detect ApoER2. This was in contrast to earlier study<sup>13</sup> showing ApoER2 expression in similar mouse line. However, this may be due to different experimental conditions since we use whole brain sample instead of hippocampal sections<sup>13</sup>.

In this study, we have consistently detected lower ApoE levels in young and aged huApoE4 TR mouse brain which concur with reduced expression of another ApoE receptor, LRP1. This ApoE-LRP1 interaction could regulate brain ApoE levels and cognitive function as conditional LRP1-KO mice experience age-dependent synaptic loss and memory decline<sup>3</sup>.

In addition, we found that the reduced ApoE expression in huApoE4 TR mice was associated with lower NR2A phosphorylation at Y1246. But, this change was not reported by earlier study<sup>13</sup> when total phosphotyrosine was probed using immunoprecipitated NR2A from hippocampal samples. Moreover, they<sup>13</sup> did not observe differential ApoE expression between huApoE4 and huApoE3 mice<sup>25–27</sup>.

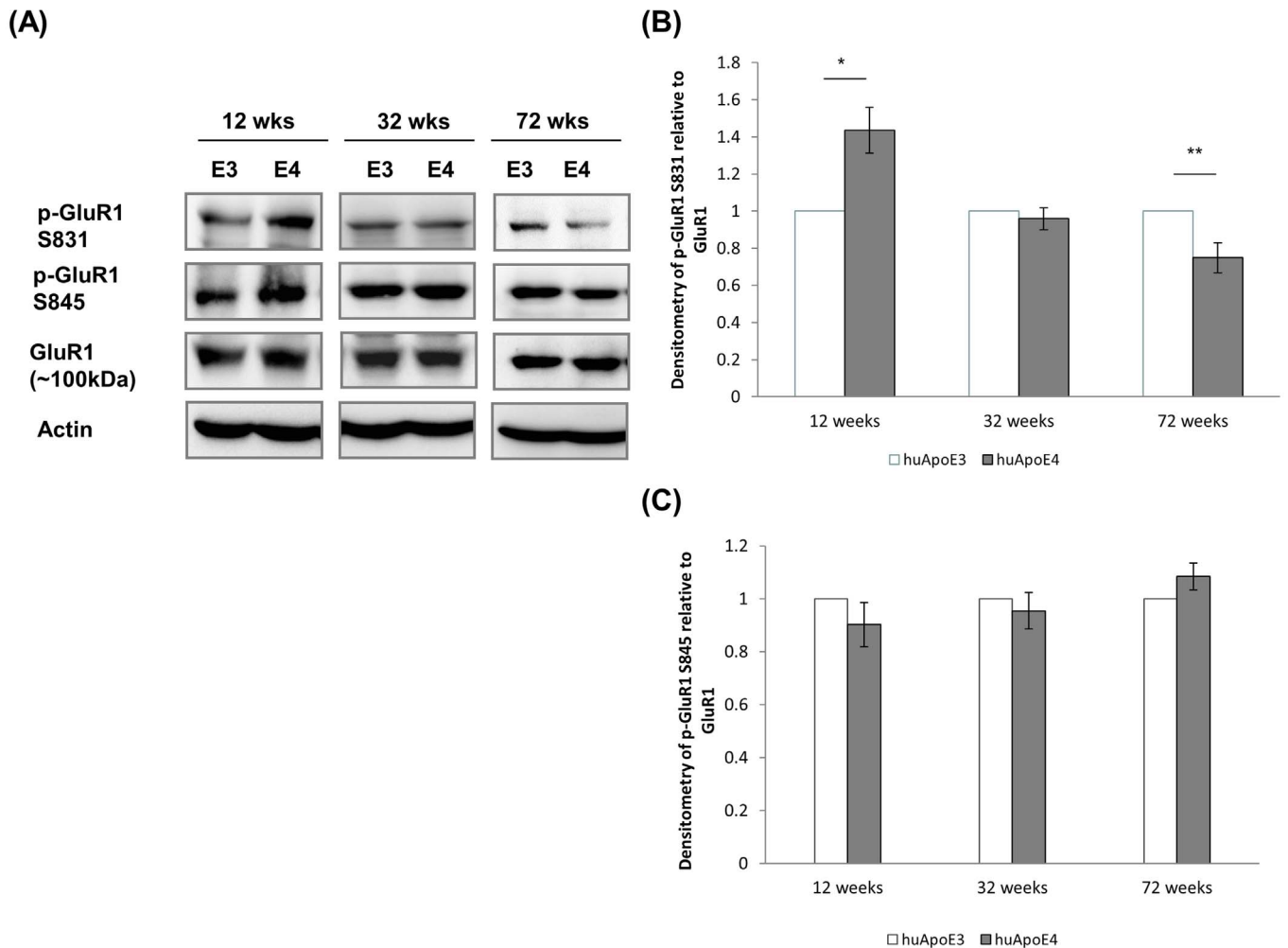


**Figure 5 | GluR1 phosphorylation at S831 but not S845 was altered in the ageing brain of huApoE TR mice.** Immunoblotting and densitometric analysis of AMPA Receptor subunit 1 (GluR1), phosphorylated GluR1 at (S831) and (S845) in E3 (white bar) and E4 (grey bar) TR mice at 12, 32 and 72 weeks of age. (A) The blot shown here is a representative of five independent experiments. Blot images were cropped for comparison. (B, C) Densitometric analysis was performed the NIH ImageJ software and the relative value for ApoE4 TR mice was normalized against age-matched ApoE3 TR mice. Each value represents the mean  $\pm$  SEM for individual mouse brain sample. (B) Brain phosphorylated GluR1 (S831) levels in E4 TR mice were significantly increased at 12 week and was significant reduced at 72 week as compared to E3 TR mice of similar age (\* $p = 0.008$ , \*\* $p = 0.01$  using Student's t-test).

ERK1/2 activation can lead to NMDAR-mediated neuroprotection in neurons<sup>36–38</sup>. We have detected increased ERK signaling in 12-week-old huApoE4 TR mice. This was also reported in earlier study<sup>13</sup> using similar mouse line at 3–5 months (~12–21 weeks).

While ApoE is mainly expressed by astrocytes, the protein can also be detected in neurons<sup>47</sup>. ApoE has been found to have a negative impact on NMDAR and AMPAR functions *in vitro*<sup>23</sup>, which affects LTP<sup>13</sup>. NR1 phosphorylation could affect AMPAR activity as these two receptors are found to co-localize in many synapses<sup>21,22</sup>. This could involve ApoE co-binding to ApoE receptor and NMDAR<sup>11</sup> leading to changes in subunit composition and/or phosphorylation as reported here.

Here, we have observed similar pattern of changes in CaMKII, PKC and GluR1 S831 phosphorylation between ApoE4 and ApoE3 mice. It is possible that GluR1 S831 phosphorylation is regulated by increased CaMKII but not PKC since the latter modulates GluR1 S845<sup>48–50</sup>.

CREB-induced synaptic activity is associated with long-term changes in neuronal plasticity which is thought to underlie learning and memory<sup>38</sup>. It is tempting to speculate that the early activation of this signal transduction may contribute to the better cognitive performance in young female ApoE4 subjects<sup>51</sup>. In contrast, reduced

neuronal signaling could be linked to the faster cognitive decline in ApoE4 non-demented subjects<sup>52,53</sup>.

Our results suggest age-specific, isoform-dependent effects of ApoE on neuronal signaling. However, there are limitations to the current study. Firstly, this study has only immunoblotted the phosphorylation proteins in the ageing mouse brain. Future interventional study using appropriate antagonists and agonists is needed to validate current observations. Another limitation is that we did not compare the age-specific, isoform-dependent effects of ApoE on neuronal signaling in different brain regions; cortex and hippocampus. This regional analysis will provide a better understanding of the molecular changes in the ageing mouse brain.

Nevertheless, this study raises an important question. While we have consistently detected lower ApoE levels in young and aged huApoE4 TR mouse brain, higher phosphorylation protein levels observed in young ApoE4 mouse brain switched to lower phosphorylation pattern in aged ApoE4 mouse brain. This suggests the involvement of other adaptor protein(s) in linking ApoE function to the NMDAR-dependent ERK/CREB signaling pathway. In addition, what is the connection between the NMDAR-associated ERK/CREB signaling and PKC activity? PKC can interact with either Ras or Raf-1, a MAPK kinase kinase (MAPKKK), and both are upstream

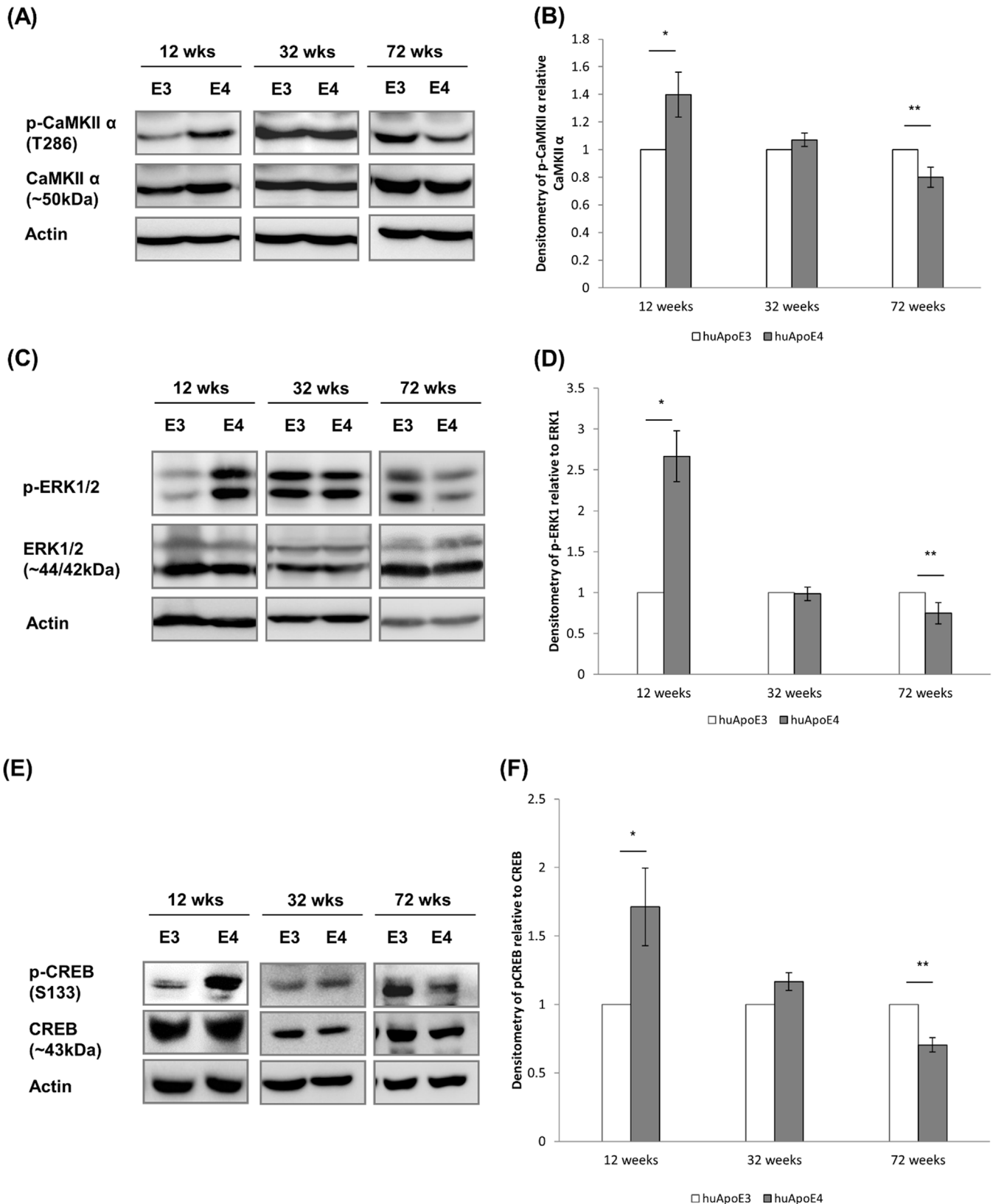


**Figure 6 | CaMKII, ERK1/2 and CREB expression and phosphorylation in the brain of huApoE4 TR mice as compared to huApoE3 TR mice.** Immunoblotting of (a) CaMKII  $\alpha$ -subunit (CaMKII $\alpha$ ), (c) ERK1/2 and (e) CREB expression and phosphorylation in E3 (white bar) and E4 (grey bar) TR mice at 12, 32 and 72 weeks of age. (A, C, E) The blot is a representative of five independent experiments. Blot images were cropped for comparison. Densitometric analysis of phosphorylated CaMKII- $\alpha$  (T286), ERK1(T202/Y204)/2(T185/Y187) and CREB (S133) was performed the NIH ImageJ software. The relative value for ApoE4 TR mice was normalized against age-matched ApoE3 TR mice. Each value represents the mean  $\pm$  SEM for individual mouse brain sample. Phosphorylated CaMKII $\alpha$ , ERK1/2 and CREB levels in E4 TR mice were significantly increased at 12 week but were significant reduced at 72 week as compared to E3 TR mice of similar age. (B) \* $p = 0.006$ , \*\* $p = 0.02$  using Student's t-test. (D) \* $p = 0.03$ , \*\* $p = 0.02$  using Student's t-test. (E) \* $p = 0.03$ , \*\* $p < 0.001$  using Student's t-test.



regulators of the ERK signaling cascade<sup>54</sup>. Further, *in vivo* ERK phosphorylation is coupled to Ca<sup>2+</sup>-dependent upstream activators including PKC and PKA in hippocampus and dorsal horn<sup>55</sup>. This warrants further investigations to unravel the intermediates that transduce NMDA signaling to downstream ERK and CREB.

## Methods

**Animals.** The animal experimental methods were carried out in accordance with the approved protocol #009/10 reviewed by the Institutional Animal Care and Use Committees (IACUC) at the National University of Singapore. The human apolipoprotein E3 and E4 targeted replacement mice were created as described<sup>56</sup> and were obtained from a colony maintained at Taconic. The endogenous mouse ApoE gene was replaced by the human APOE genomic fragments via homologous recombination. All the mice in this study were kept on 2018 Teklad Global 18% Protein Rodent Diet (Harland Laboratories). They were bred and housed conventionally, under ambient conditions (12 hrs dark, 12 hrs light). All experiments were performed on five ( $n = 5$ ) female homozygous huApoE3 and huApoE4 mice at 12, 32 and 72 weeks of age. An additional set of female homozygous mice at similar time points were used for the supplementary experiments.

**Preparation of brain homogenates.** The procedure used to prepare mouse brain homogenate is the same as described in our earlier study<sup>25</sup>. The mouse brain tissues were snapped frozen in liquid nitrogen when harvested and the wet weight of the tissues (in mg) was determined using an electronic balance. Twenty percent (w/v) brain homogenates were prepared with ice-cold 1 × RIPA lysis buffer (Cell Signaling Technology) containing detergents such as 1% Nonidet P40 and 1% sodium deoxycholate together with the protease inhibitors cocktail tablet (Roche). This lysis buffer also contains sodium orthovanadate, pyrophosphate and glycerophosphate, which can act as phosphatase inhibitors.

Lysates were homogenized using a hand held motorized pestle (Sigma-Aldrich, St. Louis, USA) for 30 seconds on ice. Tissue lysates were subsequently centrifuged at 30,000 g for 30 minutes under 4°C. The soluble portion of the lysates was collected for analysis.

**Protein quantification of lysates.** The procedure used to quantify protein concentration in mouse brain homogenates is the same as described in our earlier study<sup>25</sup>. Tissue lysates were quantified using the Pierce™ MicroBCA assay kit (ThermoFisher Scientific, Waltham, USA) in a 96-well microplate format. Lysates were diluted in PBS and the working reagent was prepared and added in accordance to the manufacturer's instructions. Samples were then incubated at 37°C for 30 minutes before reading the absorbance values at 562 nm. Protein concentrations of samples were calculated based on a standard curve constructed from a range of BSA standards. The brain tissue lysates were aliquoted and stored at -80°C.

**Immunoblot analysis.** The procedure used to perform immunoblotting is the same as described in our earlier study<sup>25</sup>. Soluble brain proteins from lysate samples were heated at 95°C for 5 minutes. Protein samples were then centrifuged at 14,000 g for 2 minutes on a bench top centrifuge before they were loaded on a 7.5% or 10% Tris-glycine polyacrylamide gel. The Precision Plus protein™ standard (Bio-Rad Laboratories, Hercules, California USA) was used as a molecular weight standard and run together with the samples on the same piece of gel.

The separated proteins were transferred onto a nitrocellulose membrane, probed with the respective primary antibodies and exposed to horseradish peroxidase (HRP)-conjugated secondary antibodies. The reactive protein bands were visualized by chemiluminescence on the Image Station 4000R (Carestream Health Inc) using the SuperSignal® West Dura Substrate (Pierce) system.

Immunoblotting of β-actin (Sigma) was included in all western blot analysis to ensure comparable protein loading. The primary antibodies used in this study were anti-huApoE (Calbiochem, Cat#178479), anti-LRP1 (Santa Cruz Biotech, Cat#SC-16168), anti-ApoER2 (Santa Cruz Biotech, Cat#SC-20746), anti-NR1 (Cell Signal Tech, Cat#5704), anti-pNR1(S896) (Cell Signal Tech, Cat#3384), anti-pNR1(S897) (Cell Signal Tech, Cat#3385), anti-NR2A (Chemicon, Cat#AB-1555), anti-pNR2A (Y1246) (Cell Signal Tech, Cat#4206), anti-NR2B (Cell Signal Tech, Cat#4207), anti-pNR2B (Y1472) (Cell Signal Tech, Cat#4208), anti-GluR1 (Cell Signal Tech, Cat#8850), anti-pGluR1(S831) (Santa Cruz Biotech, Cat#16313), anti-pGluR1(S845) (Cell Signal Tech, Cat#8084), anti-PKA-Cα (Cell Signal Tech, Cat#5842), anti-pPKA-Cα (T197) (Cell Signal Tech, Cat#5661), anti-PKCα (Abcam, Cat#ab137807), anti-pPKCα (T497) (Abcam, Cat#ab76016), anti-CaMKII (Cell Signal Tech, Cat#3357), anti-pCaMKII(T286) (Cell Signal Tech, Cat#3361), anti-ERK1/2 (Cell Signal Tech, Cat#9258), anti-pERK1/2 (Invitrogen, Cat#44689G), anti-CREB (Cell Signal Tech, Cat#9197), anti-pCREB(S133) (Cell Signal Tech, Cat#9191).

Densitometry analysis was performed<sup>25</sup> by measuring the optical densities of the targeted protein bands relative to the β-actin level from the same brain sample. For protein phosphorylation, the optical densities of the phosphorylated protein bands were measured relative to the targeted total protein level from the same brain sample. The analysis was performed using the NIH ImageJ software.

**Statistical analysis.** Significant differences were analyzed using two-tailed Student's T-test, as described in our earlier study<sup>25</sup>.

- Cosentino, S. *et al.* APOE epsilon 4 allele predicts faster cognitive decline in mild Alzheimer disease. *Neurology* **70**, 1842–1849 (2008).
- Corder, E. H. *et al.* Gene dose of apolipoprotein E type 4 allele and the risk of Alzheimer's disease in late onset families. *Science* **261**, 921–923 (1993).
- Liu, F. *et al.* The apolipoprotein E gene and its age-specific effects on cognitive function. *Neurobiol Aging* **31**, 1831–1833 (2010).
- Blair, C. K. *et al.* APOE genotype and cognitive decline in a middle-aged cohort. *Neurology* **64**, 268–276 (2005).
- Rall, S. C., Jr., Weisgraber, K. H. & Mahley, R. W. Human apolipoprotein E. The complete amino acid sequence. *J Biol Chem* **257**, 4171–4178 (1982).
- Zannis, V. I., McPherson, J., Goldberger, G., Karathanasis, S. K. & Breslow, J. L. Synthesis, intracellular processing, and signal peptide of human apolipoprotein E. *J Biol Chem* **259**, 5495–5499 (1984).
- Hartman, R. E. *et al.* Behavioral phenotyping of GFAP-*apoE3* and -*apoE4* transgenic mice: *apoE4* mice show profound working memory impairments in the absence of Alzheimer's-like neuropathology. *Exp Neurol* **170**, 326–344 (2001).
- Raber, J. *et al.* Apolipoprotein E and cognitive performance. *Nature* **404**, 352–354 (2000).
- Bu, G. Apolipoprotein E and its receptors in Alzheimer's disease: pathways, pathogenesis and therapy. *Nat Rev Neurosci* **10**, 333–344 (2009).
- Liu, C. C., Kanekiyo, T., Xu, H. & Bu, G. Apolipoprotein E and Alzheimer disease: risk, mechanisms and therapy. *Nat Rev Neurol* **9**, 106–118 (2013).
- Hoe, H. S. *et al.* Apolipoprotein E receptor 2 interactions with the N-methyl-D-aspartate receptor. *J Biol Chem* **281**, 3425–3431 (2006).
- Herz, J. & Chen, Y. Reelin, lipoprotein receptors and synaptic plasticity. *Nat Rev Neurosci* **7**, 850–859 (2006).
- Korwek, K. M., Trotter, J. H., Ladu, M. J., Sullivan, P. M. & Weeber, E. J. ApoE isoform-dependent changes in hippocampal synaptic function. *Mol Neurodegener* **4**, 21 (2009).
- Chiu, H. Y., Lin, H. H. & Lai, C. C. Potentiation of spinal NMDA-mediated nociception by cocaine- and amphetamine-regulated transcript peptide via PKA and PKC signaling pathways in rats. *Regulatory peptides* **158**, 77–85 (2009).
- Martin, A. M. *et al.* The functional role of the second NPXY motif of the LRP1 beta-chain in tissue-type plasminogen activator-mediated activation of N-methyl-D-aspartate receptors. *J Biol Chem* **283**, 12004–12013 (2008).
- Benarroch, E. E. NMDA receptors: recent insights and clinical correlations. *Neurology* **76**, 1750–1757 (2011).
- Clayton, D. A., Grosshans, D. R. & Browning, M. D. Aging and surface expression of hippocampal NMDA receptors. *J Biol Chem* **277**, 14367–14369 (2002).
- Magnusson, K. R., Nelson, S. E. & Young, A. B. Age-related changes in the protein expression of subunits of the NMDA receptor. *Brain Res Mol Brain Res* **99**, 40–45 (2002).
- Fukushima, H. *et al.* Upregulation of calcium/calmodulin-dependent protein kinase IV improves memory formation and rescues memory loss with aging. *J Neurosci* **28**, 9910–9919 (2008).
- Cohen, S. & Greenberg, M. E. Communication Between the Synapse and the Nucleus in Neuronal Development, Plasticity, and Disease. *Annu Rev Cell Dev Biol* **24**, 183–209 (2008).
- Li, B. *et al.* NMDA receptor phosphorylation at a site affected in schizophrenia controls synaptic and behavioral plasticity. *J Neurosci* **29**, 11965–11972 (2009).
- Unoki, T. *et al.* NMDA receptor-mediated PIP5K activation to produce PI(4,5)P(2) is essential for AMPA receptor endocytosis during LTD. *Neuron* **73**, 135–148 (2012).
- Chen, Y., Durakoglugil, M. S., Xian, X. & Herz, J. ApoE4 reduces glutamate receptor function and synaptic plasticity by selectively impairing ApoE receptor recycling. *Proc Natl Acad Sci U S A* **107**, 12011–12016 (2010).
- Hoe, H. S. *et al.* Effects of apoE on neuronal signaling and APP processing in rodent brain. *Brain Res* **1112**, 70–79 (2006).
- Ong, Q. R., Chan, E. S., Lim, M. L., Cole, G. M. & Wong, B. S. Reduced phosphorylation of brain insulin receptor substrate and Akt proteins in apolipoprotein-E4 targeted replacement mice. *Sci Rep* **4**, 8 (2014).
- Riddell, D. R. *et al.* Impact of apolipoprotein E (ApoE) polymorphism on brain ApoE levels. *J Neurosci* **28**, 11445–11453 (2008).
- Sullivan, P. M. *et al.* Reduced levels of human apoE4 protein in an animal model of cognitive impairment. *Neurobiol Aging* **32**, 791–801 (2011).
- Paoletti, P., Bellone, C. & Zhou, Q. NMDA receptor subunit diversity: impact on receptor properties, synaptic plasticity and disease. *Nat Rev Neurosci* **14**, 383–400 (2013).
- Raman, I. M., Tong, G. & Jahr, C. E. Beta-adrenergic regulation of synaptic NMDA receptors by cAMP-dependent protein kinase. *Neuron* **16**, 415–421 (1996).
- Tingley, W. G. *et al.* Characterization of protein kinase A and protein kinase C phosphorylation of the N-methyl-D-aspartate receptor NR1 subunit using phosphorylation site-specific antibodies. *J Biol Chem* **272**, 5157–5166 (1997).
- Montminy, M. Transcriptional regulation by cyclic AMP. *Annu Rev Biochem* **66**, 807–822 (1997).





32. Lee, H. K., Barbarosie, M., Kameyama, K., Bear, M. F. & Huganir, R. L. Regulation of distinct AMPA receptor phosphorylation sites during bidirectional synaptic plasticity. *Nature* **405**, 955–959 (2000).
33. Wang, Y., Briz, V., Chishti, A., Bi, X. & Baudry, M. Distinct Roles for mu-Calpain and m-Calpain in Synaptic NMDAR-Mediated Neuroprotection and Extrasynaptic NMDAR-Mediated Neurodegeneration. *J Neurosci* **33**, 18880–18892 (2013).
34. Hoeflich, K. P. & Ikura, M. Calmodulin in action: diversity in target recognition and activation mechanisms. *Cell* **108**, 739–742 (2002).
35. Roche, K. W., O'Brien, R. J., Mammen, A. L., Bernhardt, J. & Huganir, R. L. Characterization of multiple phosphorylation sites on the AMPA receptor GluR1 subunit. *Neuron* **16**, 1179–1188 (1996).
36. Wan, X. Z. *et al.* Activation of NMDA receptors upregulates a disintegrin and metalloproteinase 10 via a Wnt/MAPK signaling pathway. *J Neurosci* **32**, 3910–3916 (2012).
37. Xiao, L., Hu, C., Feng, C. & Chen, Y. Switching of N-methyl-D-aspartate (NMDA) receptor-favorite intracellular signal pathways from ERK1/2 protein to p38 mitogen-activated protein kinase leads to developmental changes in NMDA neurotoxicity. *J Biol Chem* **286**, 20175–20193 (2011).
38. Sakamoto, K., Karelina, K. & Obrietan, K. CREB: a multifaceted regulator of neuronal plasticity and protection. *J Neurochem* **116**, 1–9 (2011).
39. Makhinson, M., Chotiner, J. K., Watson, J. B. & O'Dell, T. J. Adenylyl cyclase activation modulates activity-dependent changes in synaptic strength and Ca<sup>2+</sup>/calmodulin-dependent kinase II autophosphorylation. *J Neurosci* **19**, 2500–2510 (1999).
40. Raber, J. *et al.* Isoform-specific effects of human apolipoprotein E on brain function revealed in ApoE knockout mice: increased susceptibility of females. *Proc Natl Acad Sci U S A* **95**, 10914–10919 (1998).
41. Wang, C. *et al.* Human apoE4-targeted replacement mice display synaptic deficits in the absence of neuropathology. *Neurobiol Dis* **18**, 390–398 (2005).
42. Holtzman, D. M., Herz, J. & Bu, G. Apolipoprotein e and apolipoprotein e receptors: normal biology and roles in Alzheimer disease. *Cold Spring Harbor perspectives in medicine* **2**, a006312 (2012).
43. Grootendorst, J. *et al.* Human apoE targeted replacement mouse lines: h-apoE4 and h-apoE3 mice differ on spatial memory performance and avoidance behavior. *Behav Brain Res* **159**, 1–14 (2005).
44. Leung, L. *et al.* Apolipoprotein E4 causes age- and sex-dependent impairments of hilar GABAergic interneurons and learning and memory deficits in mice. *PLoS One* **7**, e53569 (2012).
45. Weeber, E. J. *et al.* Reelin and ApoE receptors cooperate to enhance hippocampal synaptic plasticity and learning. *J Biol Chem* **277**, 39944–39952 (2002).
46. Brodbeck, J. *et al.* Structure-dependent impairment of intracellular apolipoprotein E4 trafficking and its detrimental effects are rescued by small-molecule structure correctors. *J Biol Chem* **286**, 17217–17226 (2011).
47. Huang, Y. & Mucke, L. Alzheimer mechanisms and therapeutic strategies. *Cell* **148**, 1204–1222 (2012).
48. Lan, J. Y. *et al.* Protein kinase C modulates NMDA receptor trafficking and gating. *Nat Neurosci* **4**, 382–390 (2001).
49. Nayak, A., Zastrow, D. J., Lickteig, R., Zahniser, N. R. & Browning, M. D. Maintenance of late-phase LTP is accompanied by PKA-dependent increase in AMPA receptor synthesis. *Nature* **394**, 680–683 (1998).
50. Sen, A., Alkon, D. L. & Nelson, T. J. Apolipoprotein E3 (ApoE3) but not ApoE4 protects against synaptic loss through increased expression of protein kinase C epsilon. *J Biol Chem* **287**, 15947–15958 (2012).
51. Yu, Y. W., Lin, C. H., Chen, S. P., Hong, C. J. & Tsai, S. J. Intelligence and event-related potentials for young female human volunteer apolipoprotein E epsilon4 and non-epsilon4 carriers. *Neurosci Lett* **294**, 179–181 (2000).
52. Filippini, N. *et al.* Differential effects of the APOE genotype on brain function across the lifespan. *Neuroimage* **54**, 602–610 (2011).
53. Greenwood, P. M., Sunderland, T., Friz, J. L. & Parasuraman, R. Genetics and visual attention: selective deficits in healthy adult carriers of the epsilon 4 allele of the apolipoprotein E gene. *Proc Natl Acad Sci U S A* **97**, 11661–11666 (2000).
54. Sweatt, J. D. The neuronal MAP kinase cascade: a biochemical signal integration system subserving synaptic plasticity and memory. *J Neurochem* **76**, 1–10 (2001).
55. Ji, R. R., Gereau, R. W. T., Malcangio, M. & Strichartz, G. R. MAP kinase and pain. *Brain Res Rev* **60**, 135–148 (2009).
56. Sullivan, P. M. *et al.* Targeted replacement of the mouse apolipoprotein E gene with the common human APOE3 allele enhances diet-induced hypercholesterolemia and atherosclerosis. *J Biol Chem* **272**, 17972–17980 (1997).

## Acknowledgments

We thank Ms H'ng Shiau Chen for her technical assistance with the supplementary experiments. This work was supported by grants to BSW from the Biomedical Research Council (BMRC/05/11/21/19/401). SMY was supported by graduate scholarship from Singapore Ministry of Education. The funders had no role in study design, data collection and analysis, decision to publish, or preparation of the manuscript.

## Author contributions

S.M.Y. and M.L.L. performed the experiments. S.M.Y. and B.S.W. conceived and designed the experiments, and analyzed the data. S.M.Y., C.M.L. and B.S.W. wrote the paper.

## Additional information

**Supplementary information** accompanies this paper at <http://www.nature.com/scientificreports>

**Competing financial interests:** The authors declare no competing financial interests.

**How to cite this article:** Yong, S.-M., Lim, M.-L., Low, C.-M. & Wong, B.-S. Reduced neuronal signaling in the ageing apolipoprotein-E4 targeted replacement female mice. *Sci. Rep.* **4**, 6580; DOI:10.1038/srep06580 (2014).



This work is licensed under a Creative Commons Attribution-NonCommercial-ShareAlike 4.0 International License. The images or other third party material in this article are included in the article's Creative Commons license, unless indicated otherwise in the credit line; if the material is not included under the Creative Commons license, users will need to obtain permission from the license holder in order to reproduce the material. To view a copy of this license, visit <http://creativecommons.org/licenses/by-nc-sa/4.0/>